ISSN 1070-3284, Russian Journal of Coordination Chemistry, 2023, Vol. 49, No. 9, pp. 612–621. © The Author(s), 2023. This article is an open access publication.

Synthesis and Antiproliferative Activity of New Copper, Cobalt, and Zinc Complexes with Abiraterone Acetate

T. A. Antonenko[a], *, Yu. A. Gracheva[a], A. V. Zazdravnykh[a], D. M. Mazur[a], D. B. Shpakovsky[a], K. A. Lyssenko[a], and E. R. Milaeva[a]

[a] *Lomonosov Moscow State University, Department of Chemistry, Moscow, Russia*

**e-mail: taisiya.antonenko@mail.ru*

Received April 4, 2023; revised April 24, 2023; accepted May 4, 2023

Abstract—New complexes $CuCl_2[AbAc]_2$ (**I**), $CoCl_2[AbAc]_2$ (**II**), and $ZnCl_2[AbAc]_2$ (**III**) with abiraterone acetate (AbAc) are synthesized. The molecular structure of complex **II** is determined by X-ray diffraction (XRD) (CIF file CCDC no. 2252346). The cobalt atom coordinates with abiraterone acetate due to the N-donor pyridine atom. The model processes of hydrolysis of the compounds in acidic and neutral media and their ability to interact with the superoxide radical anion generated in the xanthine–xanthine oxidase enzymatic system are studied. A high activity of complexes **I** and **II** is found. The MTT test shows that the antiproliferative activity of compounds **I**–**III** against the HCT-116, MCF-7, A-549, and WI-38 cells is comparable with the activity of cisplatin and exceeds that of the initial AbAc for the PC-3 cell line. Complex **II** also induces cell cycle arrest in the G0/G1 phase of RNA protein synthesis.

Keywords: metal complexes, copper, cobalt, zinc, abiraterone acetate, XRD, antiproliferative activity, cell cycle

DOI: 10.1134/S1070328423600547

INTRODUCTION

Malignant tumors are classified as socially significant pathologies. Platinum drugs (cisplatin, carboplatin, and oxaliplatin) are widely used for cancer treatment at late stages. Nevertheless, their clinical efficiency is substantially restricted by high toxicity, considerable side effects, and resistance of some types of cancer. Therefore, rapt attention is recently given to the search for drugs based on compounds of other metals. The Cu(II), Co(II), and Zn(II) complexes are known to have a broad range of biological activity. For instance, the Co(II) and Cu(II) complexes with 2-nitrobenzaldehyde glycine and 2-nitrobenzaldehyde methionine are efficient antimicrobial agents [1]. Copper is involved in many physiological cell processes and characterized by cytotoxicity [2, 3]. The copper complexes can selectively inhibit the cancer cell growth and induce apoptosis via the mitochondrial route [4] suppressing antiapoptotic proteins [5] or via the accumulation of reactive oxygen metabolites (ROM) [6, 7]. The Cu(II) bis[*N*-(*p*-tolyl)imino]acenaphthene complexes and the Cu(II) and Zn(II) complexes bearing Schiff bases were studied in vitro and in vivo on Ehrlich ascites carcinoma cells of Swiss albino mice [8]. The ability of these compounds to elongate the mice life, decrease the average tumor weight, and inhibit the tumor cell growth was found. The Cu(II) and Co(II) complexes with the imidazole-4-acetate anion have antifungal and antitumor activity [9]. In addition, the capability of these complexes of interacting with DNA was revealed. The Zn(II) complexes with 2-acetylpyridine-1-(4-fluorophenyl)piperazinyl thiosemicarbazone manifest a high antiproliferative activity, and tumor cell proliferation is achieved by blocking cell cycle progress in the S phase [10]. The acenaphthenequinone-based complexes of bis(thiosemicarbazone)zinc fluoresce and exhibit cytotoxicity (compared to that of cisplatin) on the MCF-7 cell line (human breast cancer) [11].

Prostate carcinoma (PC) is the second in abundance oncological disease and the fifth in significance cause of men death because of cancer all over the world (6.6% of the total number of deaths), and the frequency of revealing PC for men younger than 50 years continues to increase, but causes of this tendency remain unrevealed yet [12, 13]. When diagnosing at the early stage, surgical interference or radiotherapy can exert a curative effect, but metastatic castration-resistant prostate cancer (mCRPC) develops in some patients [14]. One of the methods for mCRPC treatment is abiraterone acetate (AbAc) as a prodrug of abiraterone. The latter is a perorally accessible inhibitor of the enzyme complex cytochrome P450 c17 (CYP17A1), which is the crucially important participant of androgen synthesis. Abiraterone selectively and irreversibly inhibits 17 alpha-hydroxylase/C17,

20-liase, which is the key enzyme of androgen biosynthesis [15, 16], and suppresses adrenal and tumor androgens [17, 18]. The photoactive Ru(II) complexes are also known: they liberate abiraterone under the visible light action in prostate cancer cells [19]. The photoinduced liberation results in abiraterone binding with the CYP17A1 target in the inhibitory regime.

The synthesis and antiproliferative properties of the new copper, cobalt, and zinc complexes with abiraterone acetate are presented in this work. Their stability and capability of interacting with the superoxide radical anion were also studied.

EXPERIMENTAL

Commercially available $CuCl_2 \cdot 2H_2O$, $CoCl_2$, $ZnCl_2$, abiraterone acetate (Farmoslavl', 97%), acetone (Sigma-Aldrich, 95%), and ethanol (Sigma-Aldrich, 98%) were used. Solvents were used as received.

^1H and ^{13}C NMR spectra were recorded on a Bruker AMX-400 spectrometer in $CDCl_3$ (^1H, 400 MHz; ^{13}C, 100 MHz). IR spectra were recorded on an IR 200 FT-IR spectrophotometer (Thermo-Nikolet) in KBr pellets. The synthesized compounds were analyzed by mass spectrometry with electrospray ionization (ESI) on a TSQ Endura instrument (Thermo Fisher Scientific, Waltham, MA, USA). Solutions of the complexes in acetonitrile were directly injected through a syringe pump into the ionization source with a rate of 5–10 μL/min. The spectra were recorded in the positive ion detection mode with a voltage on the source of 3.4 kV in the range m/z 150–1400. The experiment was monitored and the data were processed using the Xcalibur software.

Elemental analysis was carried out on a Vario Microcube (Elementar) C,H,N analyzer. Melting points were determined by the capillary method on a Stuart SMP10 instrument (Bibby Scientific Limited Stone, UK). The ability of the compounds to neutralize the superoxide radical anion $O_2^{-\bullet}$ generated in the xanthine–xanthine oxidase enzymatic system was determined using a Multiskan Go plate (96 wells) spectrophotometer (Thermo Fisher Sci., USA). The MTT test was conducted on a Zenyth200rt (Anthos) plate reader.

Synthesis of $CuCl_2[AbAc]_2$ (I). A solution of $CuCl_2 \cdot 2H_2O$ (50 mg, 0.29 mmol) in EtOH (9 mL) was added to a solution of AbAc (230 mg, 0.59 mmol) in acetone (4 mL). The reaction mixture was stirred at room temperature for 3 h. The solvents were removed in vacuo. The synthesized substance was washed with distilled water on a paper filter and dried in air. The yield of compound **I** as an orange-brown powder was 225 mg (84%), T_{decomp} = 139–140°C.

For $C_{52}H_{66}N_2O_4Cl_2Cu$			
Anal. calcd., %	C, 68.07	H, 7.25	N, 3.05
Found, %	C, 67.91	H, 7.12	N, 2.87

IR (KBr; ν, cm^{-1}): 3036 w, 2932 w, 1728 s, 1373 m, 1237 s, 1032 s, 797 m, 697 m, 576 w. MS (ESI): m/z 845 $[M\text{-}2Cl]^+$.

Synthesis of $CoCl_2[AbAc]_2$ (II). A solution of anhydrous $CoCl_2$ (50 mg, 0.39 mmol) in EtOH (8 mL) was added to a solution of AbAc (302 mg, 0.77 mmol) in acetone (5 mL). The reaction mixture was stirred at room temperature for 3 h. The solvents were removed in vacuo. The synthesized substance was washed with distilled water on a paper filter and dried in air. The yield of compound **II** as a bright blue powder was 267 mg (76%), T_{decomp} = 172–173°C. Bright blue crystals suitable for XRD were obtained after recrystallization from acetone.

For $C_{52}H_{66}N_2O_4Cl_2Co$			
Anal. calcd., %	C, 68.42	H, 7.29	N, 3.07
Found, %	C, 68.21	H, 7.37	N, 2.95

IR (KBr; ν, cm^{-1}): 3039 w, 2937 w, 1729 s, 1367 m, 1246 s, 1036 s, 787 m, 704 m, 691 w.

Synthesis of $ZnCl_2[AbAc]_2$ (III). A solution of anhydrous $ZnCl_2$ (20 mg, 0.15 mmol) in EtOH (6 mL) was added to a solution of AbAc (118 mg, 0.30 mmol) in acetone (3 mL). The reaction mixture was stirred at room temperature for 3 h. The solvents were removed in vacuo. The synthesized substance was washed with distilled water on a paper filter and dried in air. The yield of compound **III** as a white powder was 106 mg (77%), T_{decomp} = 168–169°C.

For $C_{52}H_{66}N_2O_4Cl_2Zn$			
Anal. calcd., %	C, 67.93	H, 7.24	N, 3.05
Found, %	C, 67.78	H, 7.09	N, 2.94

IR (KBr; ν, cm^{-1}): 3035–3060 w, 2850–2964 m, 1730 s, 1373 m, 1241 s, 1032 s, 803 s, 699 s. ^1H NMR ($CDCl_3$; δ, ppm): 8.81 (s, 2H), 8.61 (d, J = 4 Hz, 2H), 7.90 (d, J = 8 Hz, 2H), 7.47 (dd, J_1 = 8 Hz, J_2 = 4 Hz, 2H), 6.12 (s, 2H), 5.42 (d, J = 4 Hz, 2H), 4.57–4.65 (m, 2H), 2.25–2.40 (m, 6H), 2.06–2.11 (m, 4H), 2.04 (s, 6H, CH_3CO_2), 1.98–2.01 (m, 2H), 1.44–1.90 (m, 18H), 1.11–1.21 (m, 4H), 1.07 (s, 6H, CH_3), 1.03 (s, 6H, CH_3). ^{13}C NMR ($CDCl_3$; δ, ppm): 170.14, 149.47, 146.05, 145.95, 139.60, 136.71, 134.61, 131.64, 124.44, 121.72, 73.35, 56.98, 49.69, 46.92, 37.68, 36.48, 36.33, 34.57, 31.53, 30.99, 29.87, 27.29, 21.03, 20.39, 18.83, 16.21.

XRD of a single crystal of compound **II** was carried out on a Bruker D8 Quest diffractometer equipped with a Photon III detector and a microfocus X-ray tube with the MoK_α wavelength (λ = 0.71073 Å) at 110 K. Data were collected in the φ and ω scan modes. A single crystal of compound **II** ($C_{52}H_{66}N_2O_4Cl_2Co$, FW = 912.89) is orthorhombic, a = 10.1390(7), b = 14.6822(12), c = 62.030(5) Å, space group $P2_12_12_1$, Z = 8, Z' = 2, μ = 5.35 cm^{-1}, $F(000)$ = 3880. Intensities of 34040 reflections were measured at 110 K, and 17355 independent reflections of them were used in further structure determination. The structure was solved by dual methods and refined by full-matrix anisotropic least squares for F^2 using the SHELXTL software [20, 21]. Positions of hydrogen atoms were calculated and included in refinement in the isotropic approximation. The final divergence factors were R_1 = 0.0922 for 17353 observed reflections, and wR_2 and GOOF for all independent reflections were 0.2348 and 1.077, respectively.

The coordinates of atoms, bond lengths, bond angles, and thermal shift parameters were deposited with the Cambridge Crystallographic Data Centre (CIF file CCDC no. 2252346; www.ccdc.cam.ac.uk/data_request/cif).

The electronic absorption spectra of solutions of the synthesized compounds were recorded at room temperature (~25°C) on an Evolution 300 cell spectrophotometer in a range of 200–750 nm. To achieve optimum absorbances, the concentration of compounds AbAc, **II**, and **III** in acetone solutions was 2 mM, and that of compound **I** in an acetone solution was 0.1 mM.

The compounds were studied in buffer media (phosphate buffer, pH 5.5, pH 7.4) by spectrophotometry at room temperature (~25°C). The concentration of solutions of compounds AbAc and **I**–**III** in dimethyl sulfoxide (DMSO) was 2 mM.

Interaction with the $O_2^{-\cdot}$ superoxide radical anion. The ability of the compounds to neutralize the $O_2^{-\cdot}$ superoxide radical anion generated in the xanthine–xanthine oxidase enzymatic system was evaluated from the reduction rate of blue tetrazolium to formazan [22]. The reaction mixture contained a 40 mM carbonate buffer (2.76 mL, pH 10.0), 0.1 mM EDTA, 2.5 mM blue tetrazolium (0.03 mL), 10 mM xanthine, 0.5% bovine serum albumin (0.03 mL), and a solution (0.06 mL) of the studied compound in DMSO. Xanthine oxidase (0.04 units, 0.002 mL) was added to the reaction mixture at 25°C, and the absorbance was measured at λ_{max} = 560 nm for 300 s. The control experiment was carried out with the same volumes of DMSO without studied compounds. The measurements using six concentrations (0.05, 0.2, 0.75, 1.25, 2.5, and 5.0 mM) were conducted for each substance. All experiments were carried out in three repetitions.

The degree of inhibition was determined by the equation

$$I = \left(1 - A_i/A_0\right) \times 100\%,$$

where A_i is the absorbance in the presence of the tested compound at the end of the reaction (800 s), A_0 is the absorbance of the control solution, and IC_{50} were determined graphically from the dependence of I on the concentration of the compound using the Microsoft Excel 2016 software.

Procedure of operating with cell cultures. The cultures of human colon cancer (HCT-116), human breast carcinoma (MCF-7), human lung carcinoma (A-549), human prostate cancer (PC-3), and human diploid cell line consisting of fibroblasts (WI-38) were cultivated in the DMEM complete cultural medium under standard conditions reseeding them twice a week depending on the seeding density. For reseeding, the cells were washed down from the vial walls with 2 mL of a versene solution (0.02% EDTA), which chelates calcium ions necessary for cell adhesion due to which the cells are detached from the support. For a more complete detachment of the cell mass, the vial was placed in a CO_2 incubator for 15–20 min (the CO_2 content was 5%, T = 37°C, Galaxy 170S incubator, New Brunswick an eppendorf company, USA). A portion of the cell mass (~100 μL) was left in the cultural vial, suspended in a DMEM medium (7–8 mL), and placed in the incubator for further growth. The remained portion of the cell mass (1.5–2 mL) was neutralized by the addition of the DMEM cultural medium (5 mL), and the cells were precipitated by centrifugation (2 min, 2000 rpm, Universal 320R centrifuge, Germany). After centrifugation, the supernatant was removed and a precipitate of the cells was suspended in the cultural medium (5 mL). Then the cell mass (50 μL) was transferred into the eppendorf and dissolved in DMEM (450 μL). The number of cells was counted in a Goryaev chamber using a Magnus inversion biological microscope (Germany).

The cells were counted by the equation

$$(n \times 25)/100 \times [\![10]\!]^5 \ 1/\text{mL}.$$

For the further operation with the cell cultures, a necessary dilution was attained using a DMEM medium to reach a cell density of 5×10^4 1/mL. Then, a portion of the cell mass (190 μL) was introduced into each well of a sterile 96-well plate followed by cell cultivation for 24 h in a CO_2 incubator.

MTT test is based on the ability of living cell dehydrogenases, in particular, succinate dehydrogenase, to reduce uncolored forms of 3-(4,5-dimethylthiazol-2-yl)-2,5-diphenyltetrazole (MTT) to blue formazan soluble in DMSO. The MTT test was conducted via a published procedure [23] with minor modifications. Solutions with concentrations of 1, 0.25, 0.0625, 0.015, and 0.00375 mM in DMEM were prepared from the studied substances. If necessary, the sub-

stances were preliminarily dissolved in DMSO (the DMSO concentration was not higher than 0.5% of the final solution volume). The prepared solutions of the studied substances were introduced into a sterile planar-bottom 96-well plate containing cell cultures with 5- and 10-μL micropipettes in such a way that the final concentrations of the substance in the wells would be 50, 25, 12.5, 6.4, 3.2, 1.6, 0.8, 0.4, 0.2, and 0.1 μM. The plate with the cells and studied substances was placed in a CO_2 incubator for 72 h. Then 10 μL of a solution of MTT (5 μg/mL) were introduced into each well of the plate with the primary culture and studied substance, and incubation was conducted at 37°C for 2 h in a wet atmosphere with 5% CO_2. After 2 h of exposure, the living cells reduce yellow MTT to dark violet granules of formazan. The formazan granules were dissolved in DMSO (150 μL), and the amount of the reduced product was measured by spectrophotometry on a Zenyth 2000rt plate reader at a wavelength of 570 nm. The test results were presented as a plot of the dependence of % survived cells on the concentration of the studied substances. Cisplatin was applied as the standard. The experiments with the tested compounds were carried out in three repetitions.

RESULTS AND DISCUSSION

New complexes **I**–**III** were synthesized at room temperature from abiraterone acetate and chlorides of the corresponding metals (Scheme 1). The synthesized compounds are highly soluble in acetone, acetonitrile, and DMSO and are stable in air.

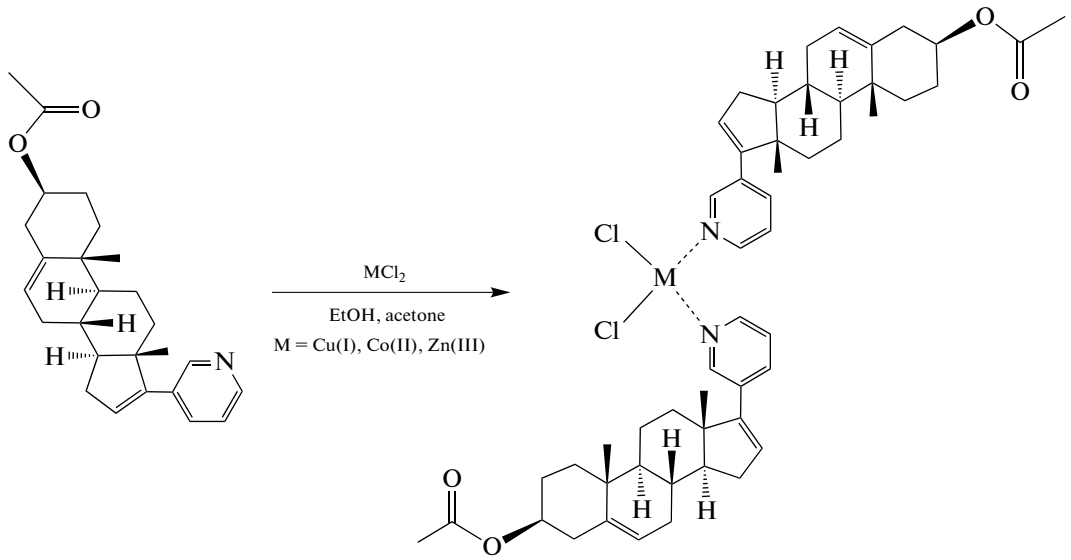

Scheme 1.

The compositions and purity of compounds **I**–**III** were confirmed by IR spectroscopy and elemental analysis, and the zinc complex was additionally studied using ^1H and ^{13}C NMR spectroscopy.

The study of the compositions of compounds **I**–**III** by mass spectrometry (ESI) showed their high sensitivity and instability under the analysis conditions. The redox processes that occur in the ionization source result in the decomposition of the starting complex and, as a consequence, the absence of the signal in the mass spectrum. Therefore, the spectra of compounds **II** and **III** exhibit only the signal of the protonated molecule of the ligand (abiraterone acetate). Some fragments of the starting compound, which were formed due to ionization, were observed only in the mass spectrum of complex **I** (Figs. 1–3). For instance, a cluster of ions, whose signal corresponds to the loss of two chlorine atoms ($[M\text{-}2Cl]^+$), was observed in the range m/z 845–849, and the range m/z 495–495 exhibits the signal of the adduct of the monoligand copper complex with acetonitrile. Probably, this is related to the formation of a stable copper(I) complex ion, whereas cobalt and zinc have no such a possibility.

The crystallization of compound **II** from acetone made it possible to obtain crystals colored in saturated blue that were used for XRD.

Since the ligand is a certain stereoisomer, the complex can crystallize only in the chiral space group, namely, in the group $P2_12_12_1$. Compound **II** crystallizes with two symmetrically independent molecules in the unit cell. The XRD study of complex **II** shows that the coordination sphere of the cobalt atom contains two ligands, both of which are bound to the metal via the pyridine nitrogen atom (Fig. 4). The coordination polyhedron of cobalt is a tetrahedron with the bond angles N(1)Co(1)N(1A) 98.6(3)°–97.1(3)° and Cl(1)Co(1)Cl(2) 116.84(10)°–116.08(11)° in two

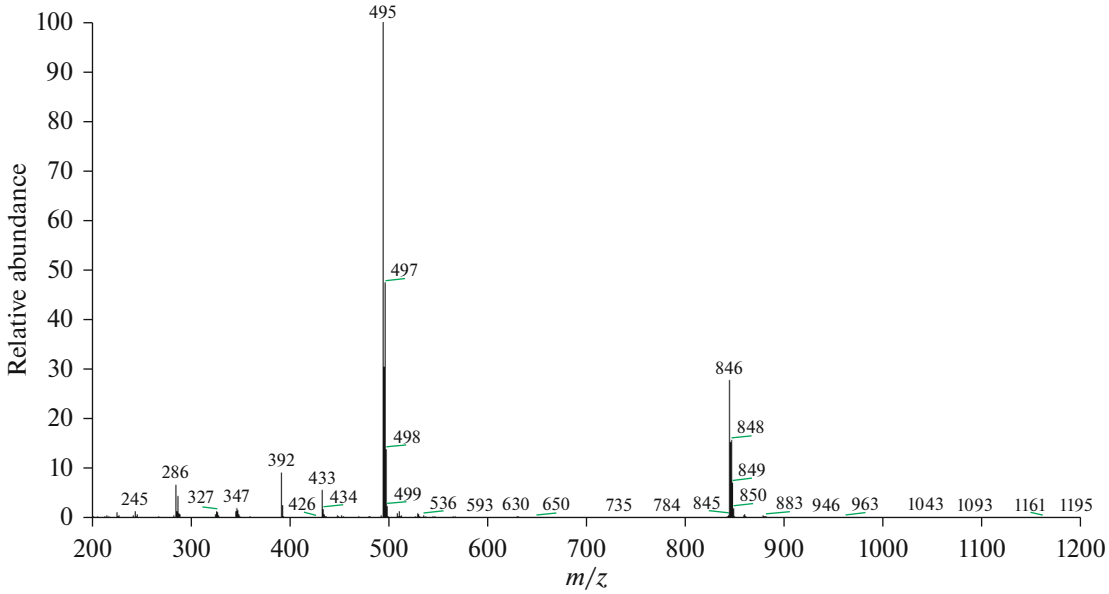

Fig. 1. Mass spectrum (ESI) of compound **I**.

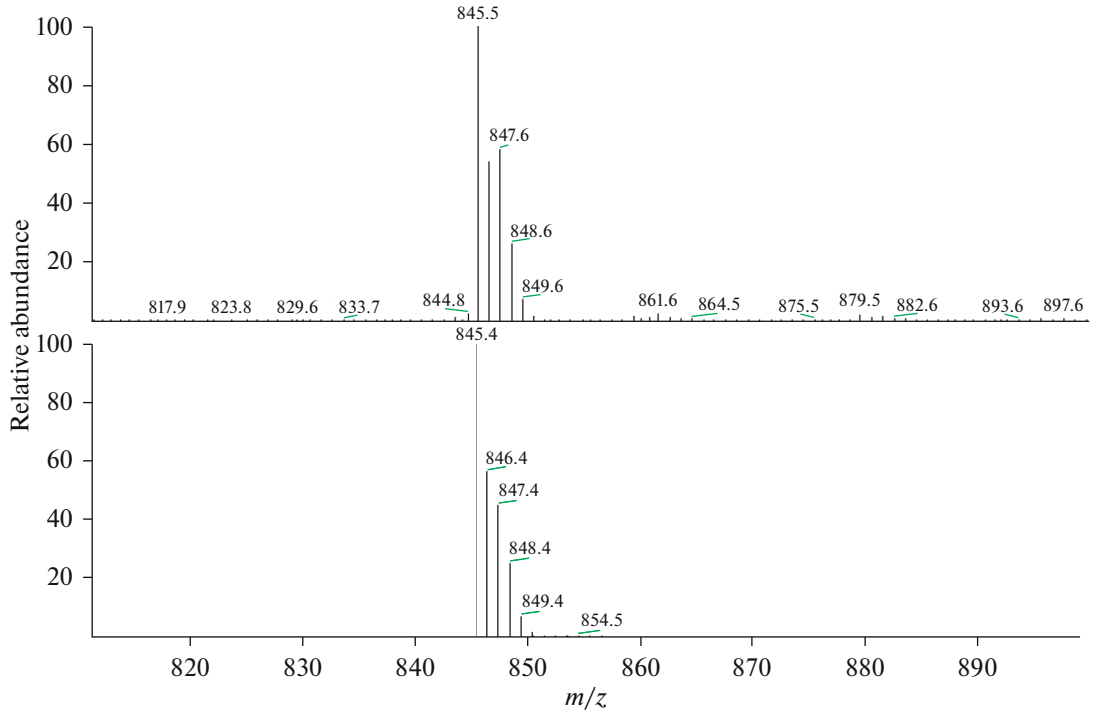

Fig. 2. Mass spectrum of compound **I** in the range m/z 820–890. Experimental cluster of ions (upper) corresponding to the loss of two chlorine atoms $[M\text{-}2Cl]^+$, and the cluster of ions simulated according to the assumed composition (bottom).

independent molecules. Although the coordination polyhedron and abiraterone itself are rather rigid, two independent molecules are different conformers that differ by the mutual turn of the pyridine rings toward each other and an insignificant variation of the mutual arrangement of the medium plane of abiraterone and the pyridine plane. The mutual turn of pyridine toward the double bond of the five-membered ring is 42.5° and 18.6° in one independent molecule and 42° and 5° in another molecule.

The studied electronic absorption spectra of solutions of the synthesized compounds in acetone in the

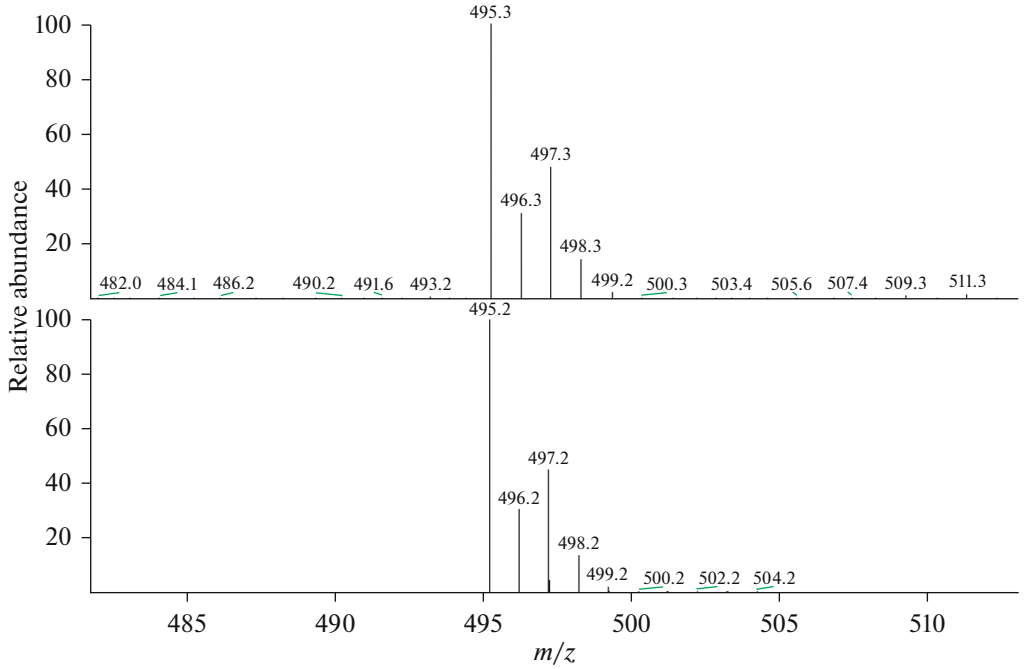

Fig. 3. Mass spectrum of compound **I** in the range m/z 485–510. Experimental cluster of ions (upper) corresponding to the adduct of the monoligand copper complex with acetonitrile, and the cluster of ions simulated according to the assumed composition (bottom).

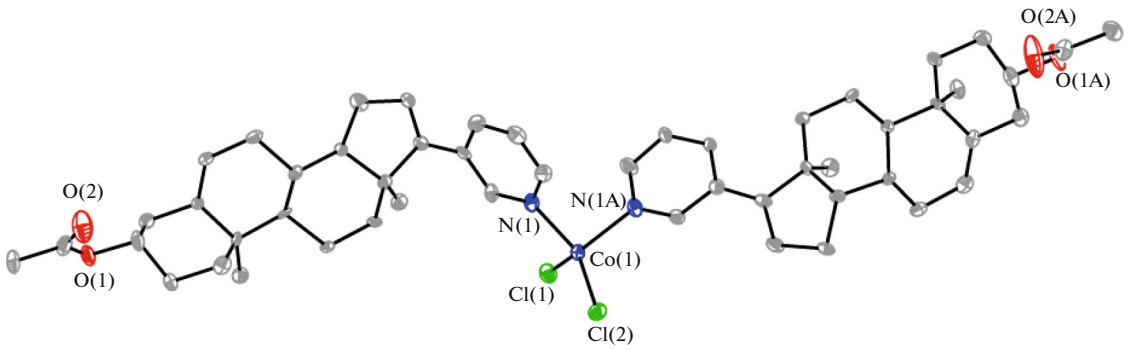

Fig. 4. General view of one of the independent molecules of compound **II** in representation of atoms by atomic shift ellipsoids (p = 50%). Hydrogen atoms are omitted.

UV and visible ranges are given in Table 1. The absorption maxima are detected in the UV range and correspond to π–π* transitions in the ligand. In the case of complex **II**, a solution of which is brightly blue, the band appears in a range of 612 nm corresponding to the *d*–*d** transition of the metal in the tetrahedral environment.

In addition, hydrolysis in cancer cells was modeled for a solution of abiraterone acetate and complexes **I**–**III** in a range of 200–750 nm (Table 1, Fig. 5) in a phosphate buffer (pH 5.5). The absorption spectra of all compounds exhibit a decrease in the absorbance in time, which is probably related to their hydrolysis.

The hydrolysis of the initial AbAc and compounds **I**–**III** was also modeled in normal cells (phosphate buffer, pH 7.4). The life-time of compounds **I**–**III** and AbAc during hydrolysis was found to be lower in an acidic medium compared to a neutral medium (Table 1, Fig. 6). In this case, copper complex **I** experiences twofold slower hydrolysis than the initial AbAc.

The antioxidant activity of compounds **I**–**III** and AbAc was evaluated from the ability to interact with the superoxide radical anion generated in the xanthine–xanthine oxidase enzymatic system. The studies were conducted by spectrophotometry from a

Table 1. Data on the electronic absorption spectra (acetone) and half-life time during hydrolysis (phosphate buffer) of compounds **I**–**III** and AbAc

Compound	λ_{1max}, nm ($\log\varepsilon_1$)	λ_{2max}, nm ($\log\varepsilon_2$)	Hydrolysis ($\tau_{1/2}$, min)	
			pH 5.5	pH 7.4
I	246 (4.09)	282 (4.10)	40	60
II	328 (2.85)	612 (1.09)	30	60
III	210 (2.76)	278 (2.46)	35	40
AbAc	248 (2.76)	254 (2.88)	20	40

change in the reduction rate of blue tetrazolium to formazan [22]. The high activity of compounds **I** and **II** was observed: IC_{50} are 43 ± 3 and 2.3 ± 0.5 μM, respectively, whereas compounds **III** and AbAc promote the formation of the superoxide radical anion. The initial $CuCl_2$ has a moderate inhibitory effect (degree of inhibition 23%). Remarkably, $CoCl_2$ exhibits no inhibitory effect compared to the pronounced activity of cobalt complex **II** and, on the contrary, promotes the formation of $O_2^{-\bullet}$.

The antiproliferative activity was studied in vitro for compounds **I**–**III** and initial AbAc on the HCT-116, MCF-7, A-549, and PC-3 cancer cells and WI-38

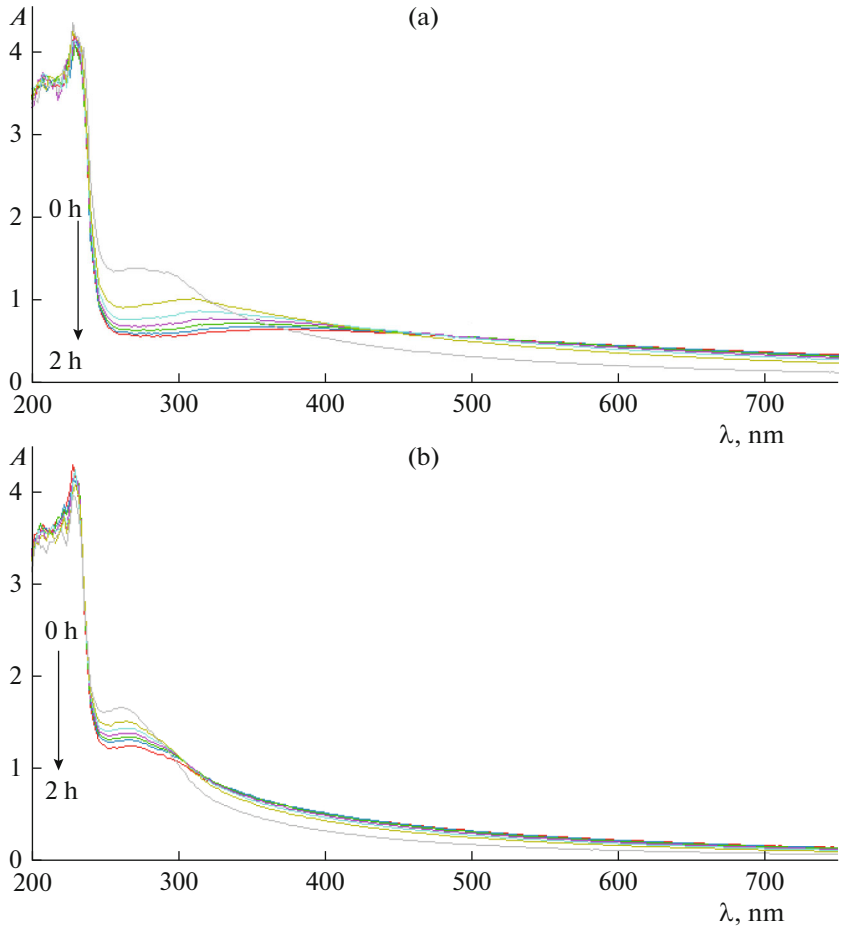

Fig. 5. Change in the absorption spectra of (a) AbAc and (b) **I** (phosphate buffer, pH 5.5). Gray color designates the absorption spectrum at the experiment onset, and the spectrum after 2 h is red.

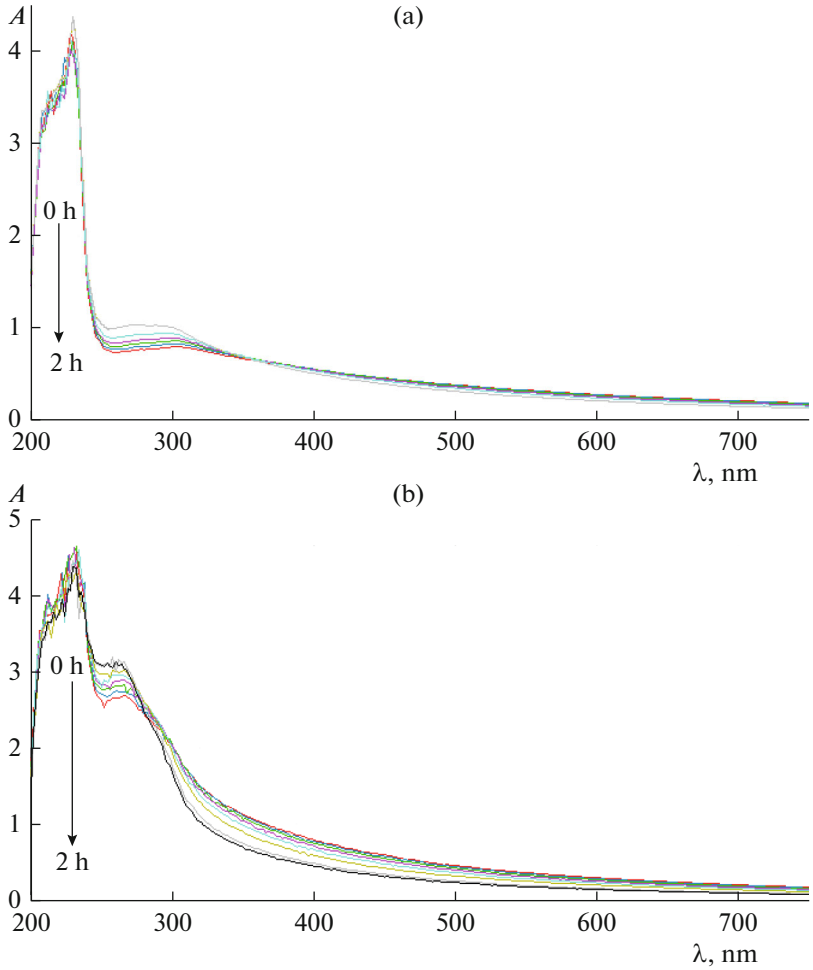

Fig. 6. Change in the absorption spectra of (a) AbAc and (b) **I** (phosphate buffer, pH 7.4). Gray color designates the absorption spectrum at the experiment onset, and the spectrum after 2 h is red.

normal cells and was compared with that of cisplatin (Table 2). The compounds manifest an activity toward the most part of the cell lines compared to that of cisplatin. Complexes **I**–**III** exhibit a higher activity against the PC-3 cells compared with that of AbAc indicating the influence of the metal on the antiproliferative properties. Compound **I** is two times more active toward this line than compounds **II** and **III**.

The influence of complex **II** on the cell cycle was tested on the HCT-116 line by the determination of the relative DNA cell content using DNA-binding fluo-

Table 2. Values of IC_{50} for compounds **I**–**III**, AbAc, and cisplatin against different cell lines

Compound	IC_{50}, μM				
	HCT-116	MCF-7	A-549	PC-3	WI-38
I	14.7 ± 1.5	12.4 ± 0.8	13.1 ± 1.2	15.8 ± 4.3	6.8 ± 2.1
II	13.1 ± 1.3	11.1 ± 0.7	13.4 ± 2.6	34 ± 7	6.2 ± 0.4
III	10.2 ± 2.4	16.6 ± 1.5	6.5 ± 2.8	32.1 ± 9.6	7 ± 3
AbAc	16 ± 4	23 ± 4	9 ± 2	>100	12.4 ± 1.7
Cisplatin	9.0 ± 0.7	7 ± 2	4.1 ± 0.7	2.2 ± 0.8	4.8 ± 0.5

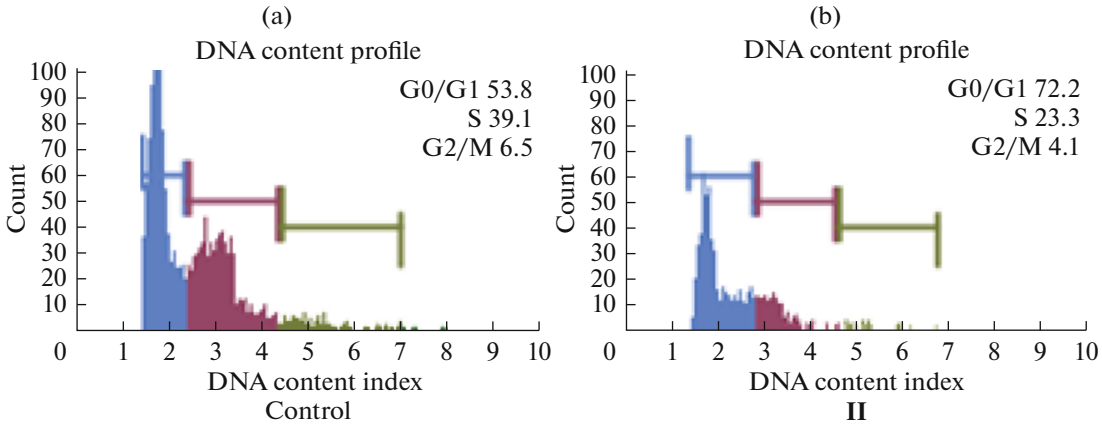

Fig. 7. Influence of compound **II** on the cell cycle of the HCT-116 cancer cell line after 48 h of incubation.

rescent dye propidium iodide. The cells were treated for 48 h with a solution of compound **II** at the concentration equal to IC_{50} in the MTT test. Cell cycle monitoring demonstrated the cell distribution between the phases of the cell cycle: G0/G1 (phase of synthesis of RNA and other cell components), S (phase of DNA replication in the karyon, centriole duplication), and G2/M (phase of preparation to mitosis/mitosis) (Fig. 7).

Complex **II** was found to cause cell cycle arrest in the G0/G1 phase of RNA protein synthesis. It is most likely that some cells exist in the reproductive dormancy state (phase G0) and undergo no fission. It is characteristic that the cells in the G0 phase are insensitive to chemotherapy. However, the stay in the dormancy phase is reversible.

Thus, new Cu (**I**), Co (**II**), and Zn (**III**) complexes with abiraterone acetate were synthesized. The molecular structure of complex **II** was determined by XRD. The stability of the initial AbAc and complexes **I**–**III** in an aqueous solution (phosphate buffer, pH 5.5 and 7.4) was studied for modeling hydrolysis in the tumor and normal cells. The capability of compounds **I**–**III** and AbAc of interacting with the superoxide radical anion generated in the xanthine–xanthine oxidase enzymatic system was studied. Compounds **I** and **II** were found to manifest a high activity. The antiproliferative properties of the compounds were studied by the MTT test. The values of IC_{50} of the synthesized compounds against the HCT-116, MCF-7, A-549, and WI-38 cells were revealed to be comparative with those for cisplatin. Compounds **I**–**III** demonstrate a higher activity on the PC-3 line compared to that of the initial AbAc. Compound **II** was also found to be capable of inducing cell cycle arrest in the G0/G1 phase of RNA protein synthesis. The results obtained provide possibilities for further studies of complexes **I**–**III** as potential anticancer agents.

ACKNOWLEDGMENTS

XRD studies were carried out on the equipment of the Center for Collective Use at the Department of Chemistry of the Moscow State University purchased in the framework of the Moscow University development program.

FUNDING

This work was supported by the Russian Science Foundation, project no. 22-23-00295.

CONFLICT OF INTEREST

The authors of this work declare that they have no conflicts of interest.

REFERENCES

1. Singh, B.K., Rajour, H.K., and Prakash, A., *Spectrochim. Acta, Part A*, 2012, vol. 94, p. 143.

2. Hussain, A., AlAjmi, M.F., Rehman, M.T., et al., *Sci. Rep.*, 2019, vol. 9, p. 1.
3. Wehbe, M., Leung, A.W., Abrams, M.J., Orvig, C., and Bally, M.B., *Dalton Trans.*, 2017, vol. 46, p. 10758.
4. Gouda, A.M., El-Ghamry, H.A., and Bawazeer, T.M., *Eur. J. Med. Chem.*, 2018, vol. 145, p. 350.
5. Fan, L., Tian, M., Liu, Y., et al., *Oncotarget*, 2017, vol. 8, p. 29823.
6. Ma, Z.Y., Qiao, Z., Wang, D.B., et al., *Appl. Organomet. Chem.*, 2017, vol. 31, p. e3651.
7. Zhang, Y.P., Ma, Z.Y., and Qiao, P.P., *Polyhedron*, 2011, vol. 193, p. 114880.
8. Raman, N., Jeyamurugan, R., Senthilkumar, R., et al., *Eur. J. Med. Chem.*, 2010, vol. 45, p. 5438.
9. Gałczyńska, K., Ciepluch, K., Madej, Ł., et al., *Sci. Rep.*, 2019, vol. 9, p. 9777.
10. Stanojkovic, T.P., Kovala-Demertzi, D., Primikyri, A., et al., *J. Inorg. Biochem.*, 2010, vol. 104, p. 467.
11. Pascu, S.I., Waghom, P.A., Conry, T.D., et al., *Dalton Trans.*, 2008, vol. 16, p. 2107.
12. Sadeghi-Gandomani, H.R., Yousefi, M.S., Rahimi, S., et al., *WCRJ*, 2017, vol. 4, p. 972.
13. Startsev, V.Yu., Shpot', E.V., Karaev, D.K., and Krivonosov, D.I., *Vest. Urolog.*, 2022, vol. 10, no. 1, p. 110.
14. Cassinello, J., Climent, M.A., Gonzalez del Alba, A., et al., *Clin. Transl. Oncol.*, 2014, vol. 16, p. 1060.
15. Attard, G., Reid, A.H.M., A'Hern, R., et al., *J. Clin. Oncol.*, 2009, vol. 27, p. 3742.
16. Ryan, C.J., Smith, M.R., Fong, L., et al., *J. Clin. Oncol.*, 2010, vol. 28, p. 1481.
17. Attard, G., Reid, A.H.M., Yap, T.A., et al., *J. Clin. Oncol.*, 2008, vol. 26, p. 4563.
18. Facchini, G., Cavaliere, C., D'Aniello, C., et al., *Anti-Cancer Drugs*, 2019, vol. 30, p. 179.
19. Li, A., Yadav, R., White, J.K., et al., *Chem. Commun.*, 2017, vol. 53, p. 3673.
20. Sheldrick, G.M., *Acta Crystallogr., Sect. A: Found. Adv.*, 2015, vol. 71, p. 3.
21. Sheldrick, G.M., *Acta Crystallogr. Sect. C: Struct. Chem.*, 2015, vol. 71, p. 3.
22. Kubo, I., Masuoka, N., Ha, T.J., and Tsujimoto, K., *Food Chem.*, 2006, vol. 99, p. 555.
23. Niks, M. and Otto, M., *J. Immunol. Methods*, 1990, vol. 130, no. 1, p. 149.

Translated by E. Yablonskaya